Local connected fractal dimension analysis in gill of fish experimentally exposed to toxicants

Maurizio MANERA, Luisa GIARI, Joseph A. DEPASQUALE, Bahram SAYYAF DEZFULI

[1]Faculty of Biosciences, Food and Environmental Technologies, University of Teramo, Piano d'Accio, I-64100 Teramo, Italy.

[2]Department of Life Sciences and Biotechnology, University of Ferrara, St. Borsari 46, I-44121 Ferrara, Italy.

[3]Morphogenyx Inc, PO Box 717, East Northport, NY 11731, USA.

Running head: Local connected fractal dimension analysis of fish gillprotein folding protein aggregation chaperone protein degradation protein metal toxicity metalloid toxicity yeast

* Correspondence: Dr. Maurizio Manera. Faculty of Biosciences, Food and Environmental Technologies, UnivWhile the toxicity of metals and metalloids, like arsenic, cadmium, mercury, lead and chromium, is undisputed, the underlying molecular mechanisms are not entirely clear. General consensus holds that proteins are the prime targets; heavy metals interfere with the physiological activity of specific, particularly susceptible proteins, either by forming a complex with functional side chain groups or by displacing essential metal ions in metalloproteins. Recent studies have revealed an additional mode of metal action targeted at proteins in a non-native state; certain heavy metals and metalloids have been found to inhibit the in vitro refolding of chemically denatured proteins, to interfere with protein folding in vivo and to cause aggregation of nascent proteins in living cells. Apparently, unfolded proteins with motile backbone and side chains are considerably more prone to engage in stable, pluridentate metal complexes than native proteins with their well-defined 3D structure. By interfering with the folding process, heavy metal ions and metalloids profoundly affect protein homeostasis and cell viability. This review describes how heavy metals impede protein folding and promote protein aggregation, how cells regulate quality control systems to protect themselves from metal toxicity and how metals might contribute to protein misfolding disorders.ersity of Teramo, Piano d'Accio, I-64100 Teramo, Italy. Telephone number:

+39 0861 266980; e-mail: mmanera@unite.it.

ABSTRACT

An operator-neutral method was implemented to objectively assess European seabass, *Dicentrarchus labrax* (Linnaeus, 1758) gill pathology after experimental exposure to cadmium (Cd) and terbuthylazine (TBA) for 24 and 48 hours. An algorithm-derived local connected fractal dimension (LCFD) frequency measure was used in this comparative analysis. Canonical variates (CVA) and linear discriminant analysis (LDA) were used to evaluate the discrimination power of the method among exposure classes (unexposed, Cd exposed, TBA exposed). Misclassification, sensitivity and specificity, both with original and cross-validated cases, were determined. LCFDs frequencies enhanced the differences among classes which were visually selected after their means, respective variances and the differences between Cd and TBA exposed means, with respect to unexposed mean, were analyzed by scatter plots. Selected frequencies were then scanned by means of LDA, stepwise analysis, and Mahalanobis distance to detect the most discriminative frequencies out of ten originally selected. Discrimination resulted in 91.7 % of cross-validated cases correctly classified (22 out of 24 total cases), with sensitivity and specificity, respectively, of 95.5 % (1 false negative with respect to 21 really positive cases) and 75 % (1 false positive with respect to 3 really negative cases). CVA with convex hull polygons ensured prompt, visually intuitive discrimination among exposure classes and graphically supported the false positive case. The combined use of semithin sections, which enhanced the visual evaluation of the overall lamellar structure; of LCFD analysis, which objectively detected local variation in complexity, without the possible bias connected to human personnel; and of CVA/LDA, could be an objective, sensitive and specific approach to study fish gill lamellar pathology. Furthermore this approach enabled discrimination with sufficient confidence between exposure classes or pathological states and avoided misdiagnosis.

Keyword: image analysis; *Dicentrarchus labrax*; sensitivity; specificity; misdiagnosis; linear discriminant analysis.

1. INTRODUCTION

Gills are the largest piscine interface with the surrounding environment, being directly and permanently in contact with potential waterborne irritants and, as a result, are suitable markers for aquatic pollution (Mallatt, 1985; Bernet et al., 1999; Manera, 2013a). Their complex structure has been described both in physiological and pathological conditions (Mallatt, 1985; Wilson and Laurent, 2002). Moreover, the pivotal role of gills in maintaining fish homeostasis, by means of gas exchange, osmoregulation, acid-base regulation, and excretion is well documented (Evans, 1987; Evans et al., 2005; Brauner and Rombough, 2012). The pathology of gills as a result of exposure to waterborne toxins has been extensively studied under both experimental conditions and in the native environment. Gills respond to a wide range of environmental physico-chemical stimuli in a limited manner and accordingly gill responses should be treated as general, though sensible, biomarkers (Mallatt, 1985; Dezfuli et al., 2006; Giari et al., 2007; Gomes et al., 2012; Nascimento et al., 2012; Wolf et al., 2015; Manera et al., 2016).

Because of their peculiar architecture, gills are intrinsically "delicate" and subject to develop artifacts during manipulations for fixation and tissue processing. This fragility leads to possible false positive/type I errors, which however can be readily dismissed provided an adequate control is available (Mallatt, 1985). In contrast, false negative/type II errors cannot be as easily dismissed. To avoid this type of error specific guides are required to correctly assess both fish gill pathology and morphometry in order to evaluate subtle gill pathological responses. False negative/type II errors, which are a greater concern than false positive /type I error should be adequately controlled by means of proper screening test sensitivity (Mallatt, 1985; Manera, 2013b-c; Szczypinski et al., 2014; Manera et al., 2016).

Fish gill assessment is currently used in environmental and ecotoxicological studies, despite the absence of any standardized method to quantify gill changes. Thus gill lesions are assessed only in a qualitative or semi-quantitative manner (Mallatt, 1985; Pawert et al., 1998; Pandey et al., 2008; Abdel-Moneim et al., 2012; Gomes et al., 2012; Nascimento et al., 2012). Nevertheless, efforts

have been made to apply metrics, indices, scores and also stereological approaches to evaluate fish gill status in environmental and toxicological studies (Pinkney et al., 1989; Lease et al., 2003; Pane et al., 2004; Alvarado et al., 2006; Monteiro et al., 2009; Agamy, 2013; Hawkins et al., 2015). Indeed, these methods rely mainly on cell counts, additional tissue elements, or reaction pattern recognition. All of these approaches are time consuming tasks and require trained personnel for operation and supervision. Not surprisingly, operator-dependent errors can arise and need to be recognized and corrected accordingly. Furthermore, to date no attempt has been made both to assess the sensitivity and the specificity of the adopted methods, and to validate the results. The authors have recently characterized branchial lamellar pathology in European seabass [*Dicentrarchus labrax* (Linnaeus, 1758)] experimentally exposed to Cadmium (Cd) and terbuthylazine (TBA), and compared the findings with unexposed cases. Guided expert quantitative and fractal analysis were performed on selected images (the same as in the present study) from resin embedded, semithin sections to test possible differences according to exposure class and the discrimination power (in term of misclassification and false positive/type I and false negative/type II errors) of the two methods, both with original and cross-validated cases, in order to obtain the respective sensitivity and specificity. Guided expert quantitative analysis was confirmed to be a reliable method to objectively characterize fish gill pathology with specific regard to toxicological trials, thus ensuring standardization and reproducibility (Manera et al., 2016). In contrast, fractal analysis alone did not approach the discrimination power that was found for guided expert analysis. Nevertheless, the authors concluded that fractal analysis deserved further investigation, because local connected fractal dimension (LCFD) analysis might prove useful in evaluating possible local variations in complexity, as opposed to the global fractal dimension utilized in that study (Manera et al., 2016). In effect, the mean global fractal dimension measurement previously used may have masked local variations in complexity, which might have been better evidenced using the LCFD analysis as proposed by Landini et al., 1995.

Fractal analysis, as an extension of conventional Euclidean geometry, constitutes a reliable method to objectively describe and summarize object complexity and heterogeneity. Fractal analysis comprises two main measures: fractal dimension, the measure of an object's complexity or its "roughness"; and lacunarity, the measure of its rotational and translational invariance or its heterogeneity and texture (Mandelbrot, 1982; Kenkel and Walker, 1996; Smith et al., 1996; Losa, 2011; West, 2013; Manera et al., 2014; Manera et al., 2016). As a simplification, fractal analysis relies on the estimation of the self-similarity properties of a fractal object, in which a portion of the same looks like the whole at different scales (Mandelbrot, 1982).

The aim of the present research was to implement an operator unbiased, objective method to comparatively assess European seabass gill pathology after exposure to Cd and TBA. The method relies on an algorithm-derived LCFD frequency measure, as opposed to a global fractal dimension measure previously performed on the same experimental material (Manera et al., 2016). Furthermore misclassification, sensitivity and specificity, both with original and cross-validated cases, were computed.

2. MATERIALS AND METHODS

The present study was based on image analysis of photomicrographs taken from a selection of semithin sections obtained in previous experimental trials (Dezfuli et al., 2006; Giari et al., 2007). In particular, all the previous histological sections compatible with the adopted image analysis, in term of tissue orientation and covered area, were included in this survey. Consequently the experimental design is only briefly summarized here and readers are referred to the cited literature.

2.1. Experimental fish and acute exposure

D. labrax specimens (mean total length, 124.4 mm; mean mass, 18.8 g; n= 45), previously acclimated for two weeks (22 ‰ salt water; mean temperature, 19.9 °C; 12 h daylight photoperiod), were exposed to four incremental doses (4.47 mg l^{-1} [0.0398 mM], 5.63 mg l^{-1} [0.0501 mM], 7.08 mg l^{-1} [0.0630 mM], 8.91 mg l^{-1} [0.0793 mM]) of Cd, and three incremental doses (3.55 mg l^{-1}

[0.0155 mM], 5.01 mg l^{-1} [0.0218 mM], 7.08 mg l^{-1} [0.0308 mM]) of TBA in 20 l polycarbonate exposure tanks, up to 48 h, while unexposed fish remained in the 200 l acclimation tank. The fish were sampled from each experimental tank after 24 and 48 h post exposure and pithed. Thereafter, their gills were gently dissected and immediately fixed in 2% glutaraldehyde solution, buffered with 0.1 M sodium cacodylate pH 7.2 at 4 °C for 2 h.

The authors emphasize that histological sections were selected from the material of previous experimental trials, whose biological assays were specifically designed to test the effects of the selected toxicants on fish tissue and cell structure, according to incremental exposure doses and exposure times. Conventional histopathological and ultrastructural screening, and cell counts were used to evaluate these samples (Dezfuli et al., 2006; Giari et al., 2007). In the present study the aim was to test the discriminant power, both in terms of sensitivity and specificity, of an operator unbiased, objective method to comparatively assess European seabass gill pathology, after exposure to Cd and TBA, irrespective to exposure dose and time. Readers interested in the effect of toxicants exposure dose and time are referred to the previous studies (Dezfuli et al., 2006; Giari et al., 2007).

2.2. Tissue processing and histological observation

After fixation tissue was post-fixed in 1% osmium tetroxide in 0.1 M sodium cacodylate at pH 7.2 for 2 h, dehydrated in a graded series of ethanol, transferred to propylene oxide and embedded in an Epon-Araldite mixture. Semithin sections (1.5 μm) were cut with a Reichert Om U2 (Reichert Optische Werke A.G., Wien, Austria) ultramicrotome with glass knives and stained with toluidine blue. Semithin sections were then observed and photographed with a microscope (Nikon Eclipse 80i; Nikon, Tokyo, Japan) equipped with a digital colour camera (DS-5M; Nikon, Tokyo, Japan) manually set to ensure the same exposure parameters, light intensity, and white balancing. Selected images were saved in TIFF (Tagged Image File Format) uncompressed file format. Detailed results of microscopic and ultrastructural patterns have been previously reported elsewhere (Dezfuli et al., 2006; Giari et al., 2007).

2.3. Fractal analysis

The TIFF colour images were binary segmented using the threshold function of the open source image analysis package ImageJ (v1.50d; Rasband W., National Institute of Health, USA) at default settings. Thereafter, the outline of each segmented image was obtained by means of the appropriate binary processing routine of ImageJ. The outline was a one pixel wide line as recommended by Smith et al. (1996); it did not correspond strictly to the branchial lamellar profile (edge) and the vascular lamellar compartment was also included in the process. The reader is referred to ImageJ documentation for any further details about the segmentation and outline algorithms used (Ferreira and Rasband, 2012) and to Manera et al. (2016) for the step by step preparative procedure, from lamellar image acquisition to outline feature extraction. LCFD was computed for each outlined image with the counting algorithm of the FracLac Image J plugin (Karperien, 1999 - 2013) as mass dimension: mass $D_F=\lim_{s\to 0}\frac{ln\mu s}{ln s}$, where $\lim_{\varepsilon\to 0}$ is found as the slope of the regression line for μ_ε and ε and μ_ε is the mean pixels per box at some ε, where ε = box size or scale. In contrast to the mean global fractal dimension, LCFD is reported as frequencies distribution rather than as a unique value. Herein, frequencies distribution was scanned for LCFD values ranging from 0.0000 to 3.0000, with incremental steps of 0.0133 (as default setting). Actually, LCFD uses pixel mass from concentrically placed sampling units, using the connected set at each pixel to produce a distribution of local variation in complexity (Landini et al., 1995; Karperien, 1999 - 2013). Information about fractal analysis is available in Mandelbrot (1982), in Seuront (2009) and in Landini (2011). More information about the employed method, the online glossary/introductory guide to fractal analysis, and to FracLac ImageJ plugin is available in Karperien (1999 - 2013).

2.4. Statistical analysis

The means of the frequencies (probabilities) of LCFDs, according to exposure class (unexposed, Cd exposed, TBA exposed) and the respective variances were assessed for normality by means of Shapiro-Wilk test. The differences among the means of the frequencies of Cd exposed and TBA exposed, with respect to unexposed fish, were also tested. They were not normally distributed and therefore were tested further for significant differences according to exposure class by means of the

k-paired Friedman nonparametric test, with both asymptotic and Montecarlo exact test extension. Moreover, the scatter plots of the means frequencies (Fig. 1), of the variances (Fig. 2) and of the differences (Fig. 3), as previously defined, were plotted to ensure their prompt and intuitive visual evaluation. In particular, the frequency values of LCFDs enhancing the differences among classes were chosen (indicated with vertical dotted/dashed lines in Figures 1 to 3), in order to scan them for discriminant power in exposure class detection by means of linear discriminant analysis (LDA). Specifically, both canonical variates analysis (CVA) and traditional LDA were applied to the selected frequencies. Data normality was previously assessed by means of Shapiro-Wilk test. With regard to LDA, stepwise analysis, Mahalanobis distance and both pooled covariance matrix and separate covariance matrices were adopted in the analysis as previously reported (Manera et al., 2016). SPSS® 14.0.2 (SPSS Inc., Chicago, IL, USA) was the statistical package for data analysis.

3. RESULTS

Compared to the unexposed gill control (Figure 1a), tissue and cell shrinkage/coarctation predominated in Cd exposed fish (Figure 1b), while cellular swelling and epithelial lifting were frequently encountered in TBA exposed fish (Figure 1c). In some instances both of these characteristics were observed.

The means of the frequencies (mean ± s.d., n= 225; unexposed= 0.004444445336 ± 0.0132958137269, Cd exposed= 0.004444444515 ± 0.0136178970500, TBA exposed= 0.004444444876 ± 0.0126215871975), the respective variances (mean ± s.d., n= 225; unexposed= 0.000001042002 ± 0.0000048879813, Cd exposed= 0.000006201129 ± 0.0000240382854, TBA exposed= 0.000008232372 ± 0.0000336545476) of LCFDs and the differences among the means of the frequencies of Cd exposed and TBA exposed with respect to unexposed fish (mean ± s.d., n= 225; Cd - unexposed= -0.000000000821± 0.0025117924941, TBA - unexposed= -0.000000000460 ± 0.0017483610155) showed significant differences (Friedman paired test, $p < 0.01$) according to exposure class.

After the visual inspection of the related scatter plots (Figures 2 to 4), frequency values corresponding to the following ten LCFDs were chosen to scan them for discriminant power in exposure class detection by means of LDA: 0.9975, 1.0108, 1.0374, 1,0507, 1.1438, 1.1571, 1.1704, 1.1837, 1.3832, 1.3965. The corresponding frequencies showed visually evident gaps in the frequency distribution scatter plots, relative to means, variances and differences, as previously defined, according to exposure class. Frequency values for the selected LCFDs are indicated as vertical dotted/dashed lines in Figures 2 to 4.

LDA, stepwise analysis, Mahalanobis distance resulted in the selection of the frequencies relative to the following four LCFDs (taken from the original ten selected frequencies): 1.0108, 1.0374, 1.0507, 1.3965. They are shown as vertical (red) dotted lines in Figures 2 to 4 to distinguish them from the discarded frequencies reported as vertical (blue) dashed lines. The results of classification with correctly classified cases, test sensitivity and specificity, in both original and cross-validated, and the values of the discriminant frequencies for each case are reported in Table 1, whereas Table 2 summarizes the selected data set as means and standard error of means. In both tables, exposure time and exposure dose (mg/l – mM) are also reported, for informative purposes. Figure 5 displays the corresponding canonical discriminant function plot (CVA). Axis 1 accounts for 99.1% of the explained variance; axis 2 for the remaining 0.9%. Convex hull polygons are clearly separated along axis 1, while unexposed case n. 3 is enclosed in the convex polygon of TBA exposed cases, corresponding to the false positive case reported in Table 1. CVA plot reported data as predicted by the model, and therefore does not indicate the false negative, TBA exposed case n. 24 detected by means of LDA through cross-validation. The discriminant variables (named according to the LCFD corresponding to each of the selected frequencies) are reported as vectors. The total length of the vectors accounts for the related discriminant power and their orthogonal projection with respect to the ordination axis, for the related contribution to ordination. Interestingly, CVA plot depicts intuitively and exactly the strong separation of Cd exposed with respect to TBA exposed and unexposed cases. Indeed, Cd exposed cases lie at the opposite side with respect to TBA exposed

and unexposed cases, along the best classificatory axis. The comparatively weaker separation between TBA exposed and unexposed cases is also clearly visible. It relies on axis 2 for classification and results in both false positive/type I and false negative/type II errors, and is thus an incomplete discrimination between TBA exposed and unexposed cases.

4. DISCUSSION

We have previously reported a general association of shrinkage/curling of epithelial cells with Cd exposure and of degenerative swelling/enlargement of epithelial cells with TBA exposure (Manera et al., 2016). Cadmium toxicity may trigger protein denaturation and oxidative stress, leading to the acute coagulation of cytoplasm and subsequent distortion of epithelial cells. Cadmium disruption of the integrity of the actin cytoskeleton or interference with the function of the cadherin cell-cell adhesion molecules could also contribute to the observed pathology (see Manera et al., 2016). Protein misfolding and aggregation due to Cd action should be taken into account too (Tamás et al, 2014). TBA-induced swelling and enlargement on the other hand is likely due to the toxicant-induced failure of membrane-associated ionic pumps (see Manera et al., 2016).

LCFD analysis and CVA-LDA are reliable methods to objectively describe fish gills lesions and to discriminate with confidence among Cd and TBA exposed, and unexposed fish gills. Fractal analysis, as mean global fractal dimension, has been previously utilized by the authors on the same semithin sections. In that study guided expert quantitative and fractal analysis (on both outline and skeleton as selected features) were used to test possible differences between exposure class and the discrimination power of the two methods. Guided expert quantitative analysis resulted as a reliable method to objectively characterize fish gill pathology, ensuring standardization and reproducibility, whereas fractal analysis did not approach the same level of discrimination power. Nevertheless, the authors concluded that fractal analysis deserved further investigation and that adoption of LCFD might prove more useful to evaluate local variations in complexity, as opposed to the mean global fractal dimension evaluated in that study (Manera et al., 2016). Essentially, mean global fractal

dimension resulted in the correct classification of only 62.5 % of cross-validated cases, with 50 % of specificity (all the unexposed cases were misclassified as Cd exposed) and 100% of sensitivity (no false negative). Nevertheless, three Cd exposed cases, out of eight, were misclassified as TBA exposed cases and three TBA exposed cases, out of thirteen, as Cd exposed. In contrast, guided expert analysis resulted in the correct classification of 87.5 % of the cross-validated cases, with 91.3 % of sensitivity (two TBA exposed cases were misclassified as unexposed – false negative/type II error) and 75 % of specificity (an unexposed case was misclassified as TBA exposed – false positive/type I error) (Manera et al., 2016). Interestingly, false positive and false negative errors reported here correspond to the false positive and to one of the false negative errors of the previous study with guided expert analysis, though an even better classification resulted from LCFD scanning method. The authors previously proposed (Manera et al., 2016) that the mean global fractal dimension measurement masked local variations in complexity, an issue which was addressed in this study with LCFD analysis, and resulting in greater clarification of these complexities.

This problem was originally addressed by Landini et al. (1995), who recognized the failure of the generalized box fractal dimension to differentiate successfully between normal and occluded retinal vessels; locally low (fractal) dimensional areas were counterbalanced, on average, by high (fractal) dimensional areas. As box fractal dimension is an average measure, it was shown to be an unreliable method to evaluate retinal perfusion abnormalities. The problem was overcome by implementing a procedure conceptually based on LCFD that has since proved successful in detecting such retinal perfusion abnormalities (Landini et al., 1995). The LCFD scanning method of the FracLac plugin implements the basic ideas of Landini and colleagues (Karperien, 1999 - 2013).

Regarding test/method assessment, false negative/type II errors are a more serious concern as compared to false positive/type I errors (Mallatt, 1985; Manera, 2013b-c; Szczypinski et al., 2014; Manera et al., 2016) and, as stressed by Mallatt (1985), cannot be readily dismissed. Because false negative/type II errors affect test sensitivity, from a clinical and environmental perspective there is

always a need for greater test sensitivity to control for or avoid them (Manera et al., 2016). The topic of both type I and type II errors occurrence in the evaluation of fish gills structural changes has been extensively reviewed by Mallatt (1985). Artifacts of fixation and tissue processing, unsuitable control selection, incorrect and uneven sectioning, and post-mortem alterations were reported to affect the occurrence of false positive/type I errors. Nevertheless, provided proper controls are used, the latter error type is not of critical concern (Mallatt, 1985). Recently, Wolf et al. (2015) reviewed the topic of misclassification in fish histopathology and stressed the limited repertoire of gill pathological response to the multitudes of physico-chemical injuries as a significant cause of misinterpretation. Thus fish gills are a sensitive though nonspecific biomarker. Mallatt (1985) stressed the need for both a guide and a morphometric approach to correctly assess fish gill pathology and to avoid false negative/type II errors. Recently, the authors proposed the combined use of semithin sections, which enhanced the evaluation of the overall lamellar structure, and of guided quantitative expert analysis, which minimizes the risk of histopathological misinterpretation and permits an objective evaluation of lesions extension, as a robust, sensitive and sufficiently specific approach to study fish gill lamellar pathology. This approach effectively isolates the truly discriminant elementary pathological findings from misdiagnosis and artifacts (Manera et al., 2016). Though effective, the “guided” method by its nature requires the assistance and supervision of a trained fish pathologist, a potential limiting factor in extensive and time-consuming surveys, where the need to discriminate with confidence among exposure classes or among normal and pathological tissue is mandatory and preferable rather than the mere description of histopathological patterns.

Image analysis techniques have dramatically improved during the last decade and many image-based diagnostic methods have been made available in bio-medicine, ranging from nuclear magnetic resonance imaging, to histopathology (Herlidou-Même et al., 2003; Castellano et al., 2004; Diamond et al., 2004; Loukas and Linney, 2004; Mahmoud-Ghoneim et al., 2006; Sertel et al., 2009; Manera, 2013b-c; Strzelecki et al., 2013; Manera and Borreca, 2014; Manera et al., 2014;

Szczypinski et al., 2014; Manera et al., 2016). In pathology there is an increasing need of objective, possibly automatic, diagnostic tools that are free from operator-dependant bias and that could assist, rather than substitute, trained pathologists (Gurcan et al., 2009; Madabhushi, 2009; Al-Janabi et al., 2012). The latter could spend their time and expertise in the validation of image analysis algorithms rather than in repetitive, laborious, possibly boring and time consuming tasks (Laurinavicius et al., 2012). The morphological evaluation of fish gills is widely and effectively used in environmental and ecotoxicological studies, although a standardized method to quantify histological changes is still lacking. To date, gill lesions have been limited to qualitative or semi-quantitative analysis (Mallatt, 1985; Pawert et al., 1998; Pandey et al., 2008; Abdel-Moneim et al., 2012; Gomes et al., 2012; Nascimento et al., 2012), with the notable exception of the quantitative study of Manera et al. (2016). In effect, metrics, indices, and scores have been used to evaluate fish gill status in environmental and toxicological studies (Lease et al., 2003; Alvarado et al., 2006; Agamy, 2013; Hawkins et al., 2015). Stereological approaches have also been performed to evaluate metal toxicity in fish gills (Pinkney et al., 1989; Pane et al., 2004; Monteiro et al., 2009). Nonetheless, these methods are rather time consuming and rely on the counting of cells, evaluation of additional tissue elements, reaction pattern recognition, all of which require the supervision of trained personnel, a possible source of human bias. Indeed, no previous attempt has been made to assess both sensitivity and specificity of these methods and to validate related results. In the present study the authors have described an operator unbiased, objective method to comparatively assess fish gill pathology. Their approach relies on an algorithm-derived LCFD frequency measure, rather than on a list of predetermined pathological features which need expert identification and quantification as previously reported (Manera et al., 2016). Moreover, the obtained classification results were cross-validated.

With regard to misclassification, errors occurred only with unexposed and TBA exposed fish gill. The relative prevalence and discrimination power of epithelial coarctation, shrinkage and epithelial swelling respectively in Cd exposed and TBA exposed fish gill have been previously observed and

discussed by the authors (Manera et al., 2016). Effectively, swelling artifacts were more frequently encountered compared to coarctation artifacts, influencing the previously proposed guided expert analysis discrimination (Manera et al., 2016) and LCFD here. Cd induced physical disruption of cell-cell and cell-matrix adhesions might well explain the cell coarctation and curling previously observed by the authors (Manera et al., 2016) and can explain why Cd exposed fish gills were never miss-classified either as unexposed, or as TBA exposed fish gills. This topic certainly deserves further investigation to determine the respective pathogenesis and probable toxic mode of action both at the cellular and at the subcellular level.

5. CONCLUSIONS

The combined use of semithin sections, which enhanced the visualization of the overall lamellar structure; of LCFD analysis, which objectively detected local variation in complexity, without the possible bias connected to human personnel; and of CVA/LDA, was shown to be a robust, sensitive and specific approach to study fish gill lamellar pathology. The combined approach effectively isolates the truly discriminant specimen features and reduces the risk of misdiagnosis when evaluating exposure classes or pathological states.

ACKNOWLEDGEMENTS

The authors thank Mr. Fernando Gelli for the technical help provided during fish exposure.

REFERENCES

Abdel-Moneim AM, Abu El-Saad AM, Hussein HK, Dekinesh SI. 2012. Gill oxidative stress and histopathological biomarkers of pollution impacts in Nile tilapia from Lake Mariut and Lake Edku, Egypt. J Aquat Anim Health 24(3):148-160.

Agamy E. 2013. Sub chronic exposure to crude oil, dispersed oil and dispersant induces histopathological alterations in the gills of the juvenile rabbit fish (*Siganus canaliculatus*). Ecotoxicol Environ Saf 92:180-190.

Al-Janabi S, Huisman A, Van Diest PJ. 2012. Digital pathology: current status and future perspectives. Histopathology 61(1):1-9.

Alvarado NE, Quesada I, Hylland K, Marigómez I, Soto M. 2006. Quantitative changes in metallothionein expression in target cell-types in the gills of turbot (*Scophthalmus maximus*) exposed to Cd, Cu, Zn and after a depuration treatment. Aquat Toxicol 77(1):64-77.

Bernet D, Schmidt H, Meier W, Burkhardt-Holm P, Wahli T. 1999. Histopathology in fish: Proposal for a protocol to assess aquatic pollution. J Fish Dis 22(1):25-34.

Brauner CJ, Rombough PJ. 2012. Ontogeny and paleophysiology of the gill: New insights from larval and air-breathing fish. Respir Physiol Neurobiol 184(3):293-300.

Castellano G, Bonilha L, Li LM, Cendes F. 2004. Texture analysis of medical images. Clin Radiol 59(12):1061-1069.

Dezfuli B, Simoni E, Giari L, Manera M. 2006. Effects of experimental terbuthylazine exposure on the cells of *Dicentrarchus labrax* (L.). Chemosphere 64(10):1684-1694.

Diamond J, Anderson NH, Bartels PH, Montironi R, Hamilton PW. 2004. The use of morphological characteristics and texture analysis in the identification of tissue composition in prostatic neoplasia. Hum Pathol 35(9):1121-1131.

Evans DH. 1987. The fish gill: Site of action and model for toxic effects of environmental pollutants. Environ Health Perspect Vol. 71:47-58.

Evans DH, Piermarini PM, Choe KP. 2005. The multifunctional fish gill: Dominant site of gas exchange, osmoregulation, acid-base regulation, and excretion of nitrogenous waste. Physiol Rev 85(1):97-177.

Ferreira TA, Rasband W. 2012. The ImageJ User Guide - IJ 1.46r. http://imagej.nih.gov/ij/docs/guide

Giari L, Manera M, Simoni E, Dezfuli B. 2007. Cellular alterations in different organs of European sea bass *Dicentrarchus labrax* (L.) exposed to cadmium. Chemosphere 67(6):1171-1181.

Gomes ID, Nascimento AA, Sales A, Araújo FG. 2012. Can fish gill anomalies be used to assess water quality in freshwater Neotropical systems? Environ Monit Assess 184(9):5523-5531.

Gurcan MN, Boucheron L, Can A, Madabhushi A, Rajpoot N, Yener B. 2009. Histopathological Image Analysis: A Review. IEEE Rev Biomed Eng 2:147-171.

Hawkins AD, Thornton C, Kennedy AJ, Bu K, Cizdziel J, Jones BW, Steevens JA, Willett KL. 2015. Gill Histopathologies Following Exposure to Nanosilver or Silver Nitrate. J Toxicol Environ Health A 78(5):301-315.

Herlidou-Même S, Constans JM, Carsin B, Olivie D, Eliat PA, Nadal-Desbarats L, Gondry C, Le Rumeur E, Idy-Peretti I, De Certaines JD. 2003. MRI texture analysis on texture test objects, normal brain and intracranial tumors. Magn Reson Imaging 21(9):989-993.

Karperien A. 1999 - 2013. FracLac for ImageJ - http://rsb.info.nih.gov/ij/plugins/fraclac/FLHelp/Introduction.htm.

Kenkel N, Walker D. 1996. Fractals in the biological sciences. Coenoses 11:77-100.

Landini G. 2011. Fractals in microscopy. J Microsc 241(1):1-8.

Landini G, Murray PI, Misson GP. 1995. Local connected fractal dimensions and lacunarity analyses of 60 degrees fluorescein angiograms. Invest Ophthalmol 36(13):2749-2755.

Laurinavicius A, Laurinaviciene A, Dasevicius D, Elie N, Plancoulaine B, Bor C, Herlin P. 2012. Digital Image Analysis in Pathology: Benefits and Obligation. Anal Cell Pathol 35(2).

Lease HM, Hansen JA, Bergman HL, Meyer JS. 2003. Structural changes in gills of Lost River suckers exposed to elevated pH and ammonia concentrations. Comp Biochem Physiol C Toxicol Pharmacol 134(4):491-500.

Losa, G.A. 2011. Fractals in biology and medicine. Encyclo. Mol. Cell Biol. Mol. Med.

Loukas CG, Linney A. 2004. A survey on histological image analysis-based assessment of three major biological factors influencing radiotherapy: Proliferation, hypoxia and vasculature. Comput Methods Programs Biomed 74(3):183-199.

Madabhushi A. 2009. Digital pathology image analysis: opportunities and challenges. Imaging Med 1(1):7-10.

Mahmoud-Ghoneim D, Cherel Y, Lemaire L, De Certaines JD, Maniere A. 2006. Texture analysis of magnetic resonance images of rat muscles during atrophy and regeneration. Magn Reson Imaging 24(2):167-171.

Mallatt J. 1985. Fish gill structural changes induced by toxicants and other irritants: A statistical review. Can J Fish Aquat Sci 42(4):630-648.

Mandelbrot BB. 1982. The fractal geometry of nature. Oxford: Freeman.

Manera M. 2013a. I biomarcatori nel monitoraggio ambientale. Pesci ossei ed ecosistemi acquatici. Rome: Aracne.

Manera M. 2013b. RGB stacks gray-level analysis to study mast cell degranulation to intestinal contraction correlation in trout. J Morphol Sci 30(3):170-175.

Manera M. 2013c. The use of texture analysis in the morpho-functional characterization of mast cell degranulation in rainbow trout (*Onchorhynchus mykiss*). Microsc Microanal 19(6):1436-1444.

Manera M, Borreca C. 2014. The use of texture analysis in the vertebral morphometric study of a lordotic chub (*Squalius cephalus* L.). J Coast Life Med 2(8):606-608.

Manera M, Dezfuli BS, Borreca C, Giari L. 2014. The use of fractal dimension and lacunarity in the characterization of mast cell degranulation in rainbow trout (*Onchorhynchus mykiss*). J Microsc 256(2):82-89.

Manera M, Giari L, DePasquale JA, Dezfuli BS. 2016. European sea bass gill pathology after exposure to cadmium and terbuthylazine: expert versus fractal analysis. J Microsc 261(3): 291-299.

Monteiro SM, Rocha E, Mancera JM, Fontaínhas-Fernandes A, Sousa M. 2009. A stereological study of copper toxicity in gills of *Oreochromis niloticus*. Ecotoxicol Environ Saf 72(1):213-223.

Nascimento A, Araújo F, Gomes I, Mendes R, Sales A. 2012. Fish Gills Alterations as Potential Biomarkers of Environmental Quality in a Eutrophized Tropical River in South-Eastern Brazil. Anat Histol Embryol 41(3):209-216.

Pandey S, Parvez S, Ansari RA, Ali M, Kaur M, Hayat F, Ahmad F, Raisuddin S. 2008. Effects of exposure to multiple trace metals on biochemical, histological and ultrastructural features of gills of a freshwater fish, *Channa punctata* Bloch. Chem Biol Interact 174(3):183-92.

Pane EF, Haque A, Goss GG, Wood CM. 2004. The physiological consequences of exposure to chronic, sublethal waterborne nickel in rainbow trout (*Oncorhynchus mykiss*): exercise vs resting physiology. J Exp Biol 207(7):1249-1261.

Pawert M, Müller E, Triebskorn R. 1998. Ultrastructural changes in fish gills as biomarker to assess small stream pollution. Tissue Cell 30(6):617-626.

Pinkney AE, Wright DA, Hughes GM. 1989. A morphometric study of the effects of tributyltin compounds on the gills of the mummichog, *Fundulus heteroclitus*. J Fish Biol 34(5):665-677.

Sertel O, Kong J, Catalyurek UV, Lozanski G, Saltz JH, Gurcan MN. 2009. Histopathological image analysis using model-based intermediate representations and color texture: Follicular lymphoma grading. J Sign Proc Syst 55(1-3):169-183.

Seuront L. 2009. Fractals and Multifractals in Ecology and Aquatic Science. Boca Raton: CRC Press.

Smith TG, Jr., Lange GD, Marks WB. 1996. Fractal methods and results in cellular morphology--dimensions, lacunarity and multifractals. J Neurosci Methods 69(2):123-36.

Strzelecki M, Szczypinski P, Materka A, Klepaczko A. 2013. A software tool for automatic classification and segmentation of 2D/3D medical images. Nucl Instr Meth Phys Res A 702:137-140.

Szczypinski P, Klepaczko A, Pazurek M, Daniel P. 2014. Texture and color based image segmentation and pathology detection in capsule endoscopy videos. Comput Methods Programs Biomed 113(1): 396-411.

Tamás MJ, Sharma SK, Ibstedt S, Jacobson T, Christen P. 2014. Heavy metals and metalloids as a cause for protein misfolding and aggregation. Biomolecules 4(1):2 52-267.

West BJ. 2013. Fractal Physology and Chaos in Medicine: World Scientific Publishing Company.

Wilson JM, Laurent P. 2002. Fish gill morphology: Inside out. J Exp Zool 293(3):192-213.

Wolf JC, Baumgartner WA, Blazer VS, Camus AC, Engelhardt JA, Fournie JW, Frasca S, Groman DB, Kent ML, Khoo LH and others. 2015. Nonlesions, Misdiagnoses, Missed Diagnoses, and Other Interpretive Challenges in Fish Histopathology Studies: A Guide for Investigators, Authors, Reviewers, and Readers. Toxicol Pathol 43(3):297-325.

Table 1. Classification according to linear discriminant, stepwise analysis – Mahalanobis distance. Values of the selected discriminant frequencies, and exposure time and dose (only as informative purpose) are also reported for each case.

	Case number	Exposure time (h)	Exposure dose (mg/l – mM)	1.0108	1.0374	1.0507	1.3965	Given group	Classified group	Error type
Original[a]	1	0	0	0.0567237	0.0255301	0.0372266	0.0105620	Unexposed	Unexposed	-
	2	0	0	0.0567237	0.0255301	0.0372266	0.0105620	Unexposed	Unexposed	-
	3	0	0	0.0462515	0.0285025	0.0401619	0.0118674	Unexposed	TBA exposed*	False positive – Type I
	4	24	5.63 (0.0501)	0.0586622	0.0173391	0.0380835	0.0095623	Cd exposed	Cd exposed	-
	5	24	5.63 (0.0501)	0.0396755	0.0407836	0.0679430	0.0260908	Cd exposed	Cd exposed	-
	6	24	7.08 (0.0630)	0.0514649	0.0224860	0.0435356	0.0135823	Cd exposed	Cd exposed	-
	7	24	7.08 (0.0630)	0.0487131	0.0303294	0.0522998	0.0193592	Cd exposed	Cd exposed	-
	8	24	8.91 (0.0793)	0.0430261	0.0260246	0.0487011	0.0165859	Cd exposed	Cd exposed	-
	9	24	8.91 (0.0793)	0.0368852	0.0475702	0.0742063	0.0347765	Cd exposed	Cd exposed	-
	10	24	8.91 (0.0793)	0.0377562	0.0377028	0.0666845	0.0247331	Cd exposed	Cd exposed	-
	11	48	4.47 (0.0398)	0.0575951	0.0158531	0.0320771	0.0097576	Cd exposed	Cd exposed	-
	12	48	4.47 (0.0398)	0.0422952	0.0296370	0.0559438	0.0183516	Cd exposed	Cd exposed	-

	13	48	5.63 (0.0501)	0.0400365	0.0325799	0.0582354	0.0208331	Cd exposed	Cd exposed	-
	14	48	7.08 (0.0630)	0.0507903	0.0192364	0.0390033	0.0115159	Cd exposed	Cd exposed	-
	15	48	8.91 (0.0793)	0.0598674	0.0168562	0.0336087	0.0106768	Cd exposed	Cd exposed	-
	16	48	8.91 (0.0793)	0.0407565	0.0429471	0.0622681	0.0286014	Cd exposed	Cd exposed	-
	17	24	3.55 (0.0155)	0.0399903	0.0376923	0.0515245	0.0170233	TBA exposed	TBA exposed	-
	18	24	3.55 (0.0155)	0.0548774	0.0229123	0.0328771	0.0110477	TBA exposed	TBA exposed	-
	19	24	3.55 (0.0155)	0.0432560	0.0479183	0.0649810	0.0245893	TBA exposed	TBA exposed	-
	20	24	7.08 (0.0308)	0.0602600	0.0192113	0.0286140	0.0073742	TBA exposed	TBA exposed	-
	21	48	3.55 (0.0155)	0.0481321	0.0175318	0.0281445	0.0073473	TBA exposed	TBA exposed	-
	22	48	3.55 (0.0155)	0.0454680	0.0306100	0.0429430	0.0133229	TBA exposed	TBA exposed	-
	23	48	5.01 (0.0218)	0.0459863	0.0377129	0.0512888	0.0176394	TBA exposed	TBA exposed	-
	24	48	5.01 (0.0218)	0.0399002	0.0582669	0.0709210	0.0345548	TBA exposed	TBA exposed	-
Cross-validated[b]	1	0	0	0.0567237	0.0255301	0.0372266	0.0105620	Unexposed	Unexposed	-
	2	0	0	0.0567237	0.0255301	0.0372266	0.0105620	Unexposed	Unexposed	-
	3	0	0	0.0462515	0.0285025	0.0401619	0.0118674	Unexposed	TBA exposed*	False positive – Type I
	4	24	5.63 (0.0501)	0.0586622	0.0173391	0.0380835	0.0095623	Cd exposed	Cd exposed	-
	5	24	5.63 (0.0501)	0.0396755	0.0407836	0.0679430	0.0260908	Cd exposed	Cd exposed	-

	6	24	7.08 (0.0630)	0.0514649	0.0224860	0.0435356	0.0135823	Cd exposed	Cd exposed	-
	7	24	7.08 (0.0630)	0.0487131	0.0303294	0.0522998	0.0193592	Cd exposed	Cd exposed	-
	8	24	8.91 (0.0793)	0.0430261	0.0260246	0.0487011	0.0165859	Cd exposed	Cd exposed	-
	9	24	8.91 (0.0793)	0.0368852	0.0475702	0.0742063	0.0347765	Cd exposed	Cd exposed	-
	10	24	8.91 (0.0793)	0.0377562	0.0377028	0.0666845	0.0247331	Cd exposed	Cd exposed	-
	11	48	4.47 (0.0398)	0.0575951	0.0158531	0.0320771	0.0097576	Cd exposed	Cd exposed	-
	12	48	4.47 (0.0398)	0.0422952	0.0296370	0.0559438	0.0183516	Cd exposed	Cd exposed	-
	13	48	5.63 (0.0501)	0.0400365	0.0325799	0.0582354	0.0208331	Cd exposed	Cd exposed	-
	14	48	7.08 (0.0630)	0.0507903	0.0192364	0.0390033	0.0115159	Cd exposed	Cd exposed	-
	15	48	8.91 (0.0793)	0.0598674	0.0168562	0.0336087	0.0106768	Cd exposed	Cd exposed	-
	16	48	8.91 (0.0793)	0.0407565	0.0429471	0.0622681	0.0286014	Cd exposed	Cd exposed	-
	17	24	3.55 (0.0155)	0.0399903	0.0376923	0.0515245	0.0170233	TBA exposed	TBA exposed	-
	18	24	3.55 (0.0155)	0.0548774	0.0229123	0.0328771	0.0110477	TBA exposed	TBA exposed	-
	19	24	3.55 (0.0155)	0.0432560	0.0479183	0.0649810	0.0245893	TBA exposed	TBA exposed	-
	20	24	7.08 (0.0308)	0.0602600	0.0192113	0.0286140	0.0073742	TBA exposed	TBA exposed	-
	21	48	3.55 (0.0155)	0.0481321	0.0175318	0.0281445	0.0073473	TBA exposed	TBA exposed	-
	22	48	3.55 (0.0155)	0.0454680	0.0306100	0.0429430	0.0133229	TBA exposed	TBA exposed	-

	23	48	5.01 (0.0218)	0.0459863	0.0377129	0.0512888	0.0176394	TBA exposed	TBA exposed	-
	24	48	5.01 (0.0218)	0.0399002	0.0582669	0.0709210	0.0345548	TBA exposed	Unexposed *	False negative – Type II

*Misclassified data. [a] 95.8 % of cases correctly classified; sensitivity of 100 %, specificity of 75 %. [b] 91.7 % of cases correctly classified; sensitivity of 95.5 %, specificity of 75 %.

Table 2. Summary of means and standard error of means (s.e.m.) according to exposure class. Values of exposure time and dose are also reported as informative purpose only.

Exposure class	Exposure time (h)	Exposure dose (mg/l – mM)		1.0108	1.0374	1.0507	1.3965
Unexposed	0	0.0000	N	3	3	3	3
			Mean	0.010997133	0.026520900	0.038205033	0.007687367
			S.E.M	0.000435133	0.000990800	0.000978433	0.000730966
Cd exposed	48	4.47 (0.0398)	N	2	2	2	2
			Mean	0.014054600	0.022745050	0.044010450	0.005796200
			S.E.M	0.004297000	0.006891950	0.011933350	0.000349600
	24	5.63 (0.0501)	N	2	2	2	2
			Mean	0.017826550	0.029061350	0.053013250	0.003323650
			S.E.M	0.008264250	0.011722250	0.014929750	0.000139250
	48	5.63 (0.0501)	N	1	1	1	1
			Mean	0.020833100	0.032579900	0.058235400	0.007749200
	24	7.08 (0.0630)	N				
			Mean	0.016470750	0.026407700	0.047917700	0.004045600
			S.E.M	0.002888450	0.003921700	0.004382100	0.001884600
	48	7.08 (0.0630)	N	1	1	1	1
			Mean	0.011515900	0.019236400	0.039003300	0.004314100
			S.E.M	-	-	-	-
	24	8.91 (0.0793)	N	3	3	3	3
			Mean	0.025365167	0.037099200	0.063197300	0.002909100
			S.E.M	0.005260675	0.006226996	0.007566356	0.000644218

	48	8.91 (0.0793)	N	2	2	2	2
			Mean	0.019639100	0.029901650	0.047938400	0.006266400
			S.E.M	0.008962300	0.013045450	0.014329700	0.000042600
	Total Cd exposed		N	13	13	13	13
			Mean	0.018802038	0.029180415	0.051737708	0.004588792
			S.E.M	0.002210974	0.002965003	0.003841633	0.000511056
TBA exposed	24	3.55 (0.0155)	N	3	3	3	3
			Mean	0.017553433	0.036174300	0.049794200	0.009518833
			S.E.M	0.003918099	0.007258403	0.009307891	0.002968739
	48	3.55 (0.0155)	N	2	2	2	2
			Mean	0.010335100	0.024070900	0.035543750	0.011454250
			S.E.M	0.002987800	0.006539100	0.007399250	0.001192750
	48	5.01 (0.0218)	N	2	2	2	2
			Mean	0.026097100	0.047989900	0.061104900	0.003666200
			S.E.M	0.008457700	0.010277000	0.009816100	0.001880200
	24	7.08 (0.0308)	N	1	1	1	1
			Mean	0.007374200	0.019211300	0.028614000	0.011491700
			S.E.M	-	-	-	-
	Total TBA exposed		N	8	8	8	8
			Mean	0.016612363	0.033981975	0.046411738	0.008786138
			S.E.M	0.003272606	0.005060974	0.005733855	0.001572031

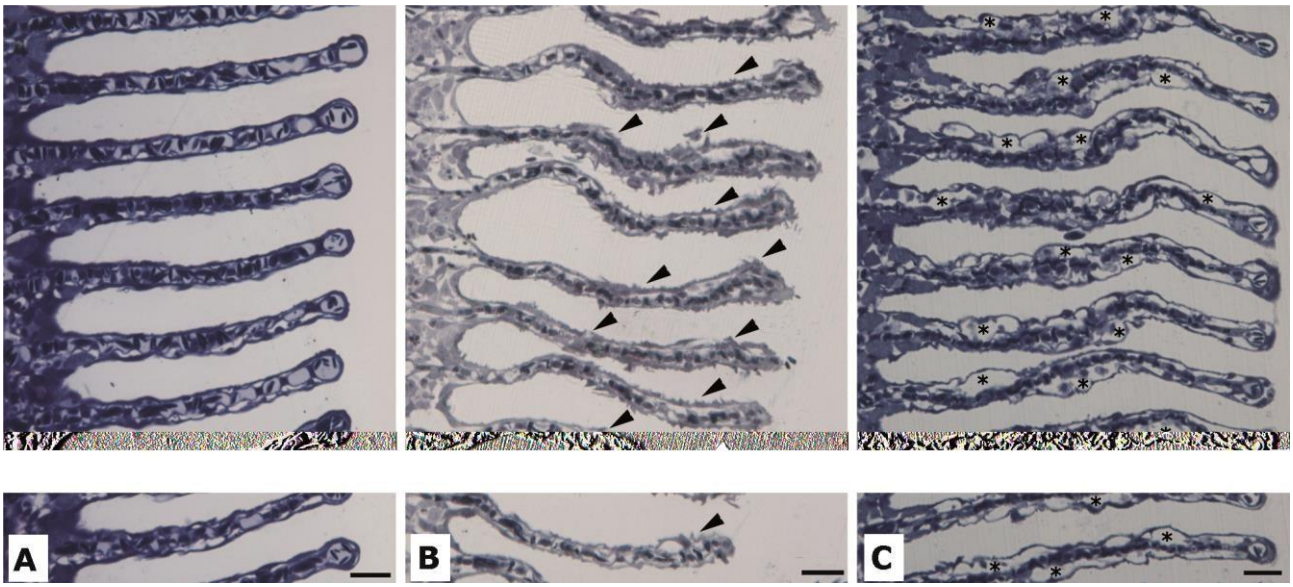

Fig. 1. European seabass. Unexposed (A), Cd exposed (B), TBA exposed (C) secondary gill lamellae. Shrinkage/curling of epithelial cells (black arrow heads) are clearly visible in Cd exposed lamellae, whereas epithelial lifting (black asterisks) occurred mainly in TBA exposed lamellae. Semithin sections. Toluidine Blue. Scale bar= 20 μm.

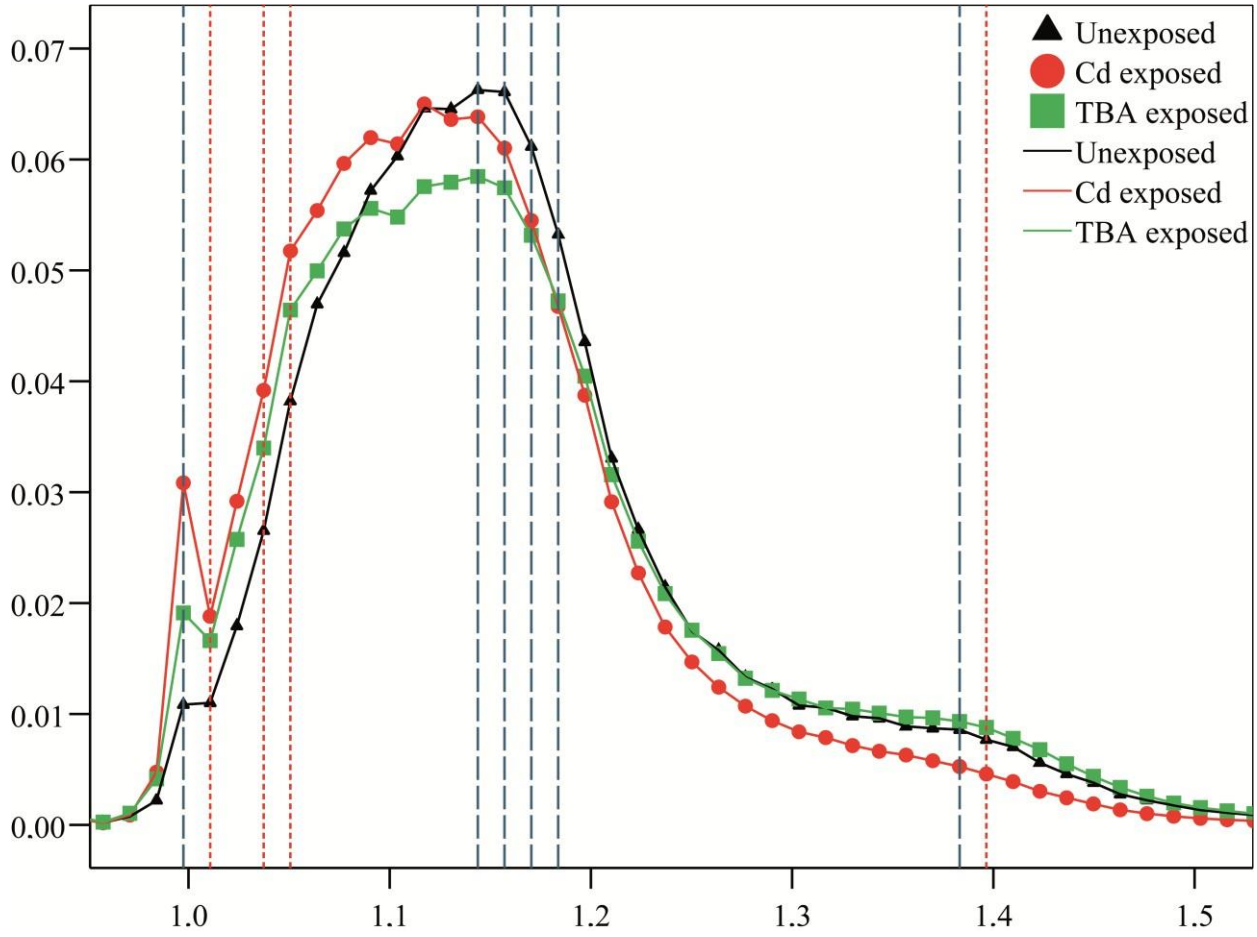

Fig. 2. Scatter plot of the mean frequencies (y axis) to LCFD (x axis), according to exposure class. The vertical dotted (red)/dashed (blue) lines demonstrates the frequency values of LCFD enhancing the differences among classes. The dotted (red) vertical lines refer to values selected by means of linear discriminant stepwise analysis.

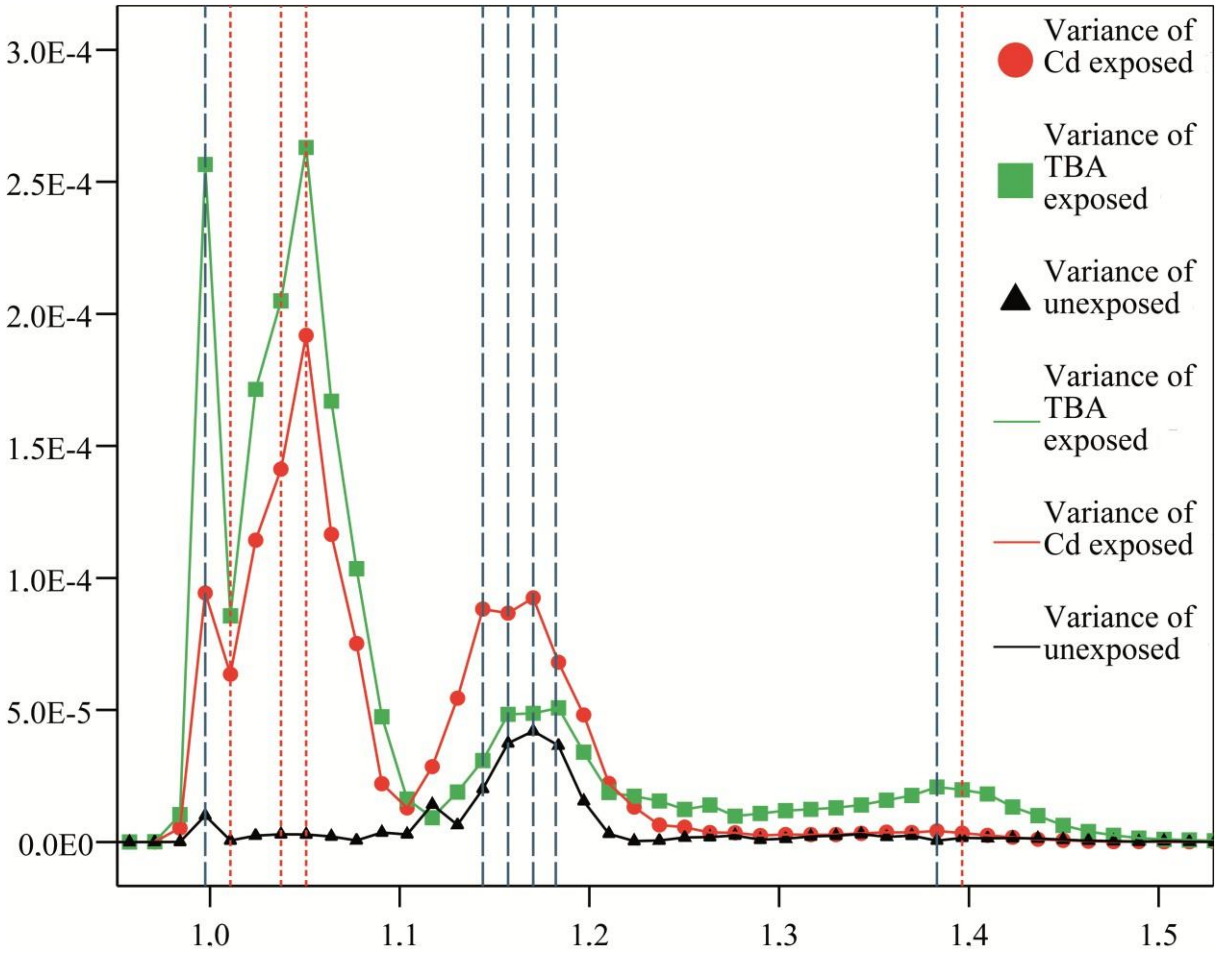

Fig. 3. Scatter plot of the variances of the mean frequencies (y axis) to LCFD (x axis), according to exposure class. The vertical dotted (red)/dashed (blue) lines demonstrates the frequency values of LCFD enhancing the differences among classes. The dotted (red) vertical lines refer to values selected by means of linear discriminant stepwise analysis.

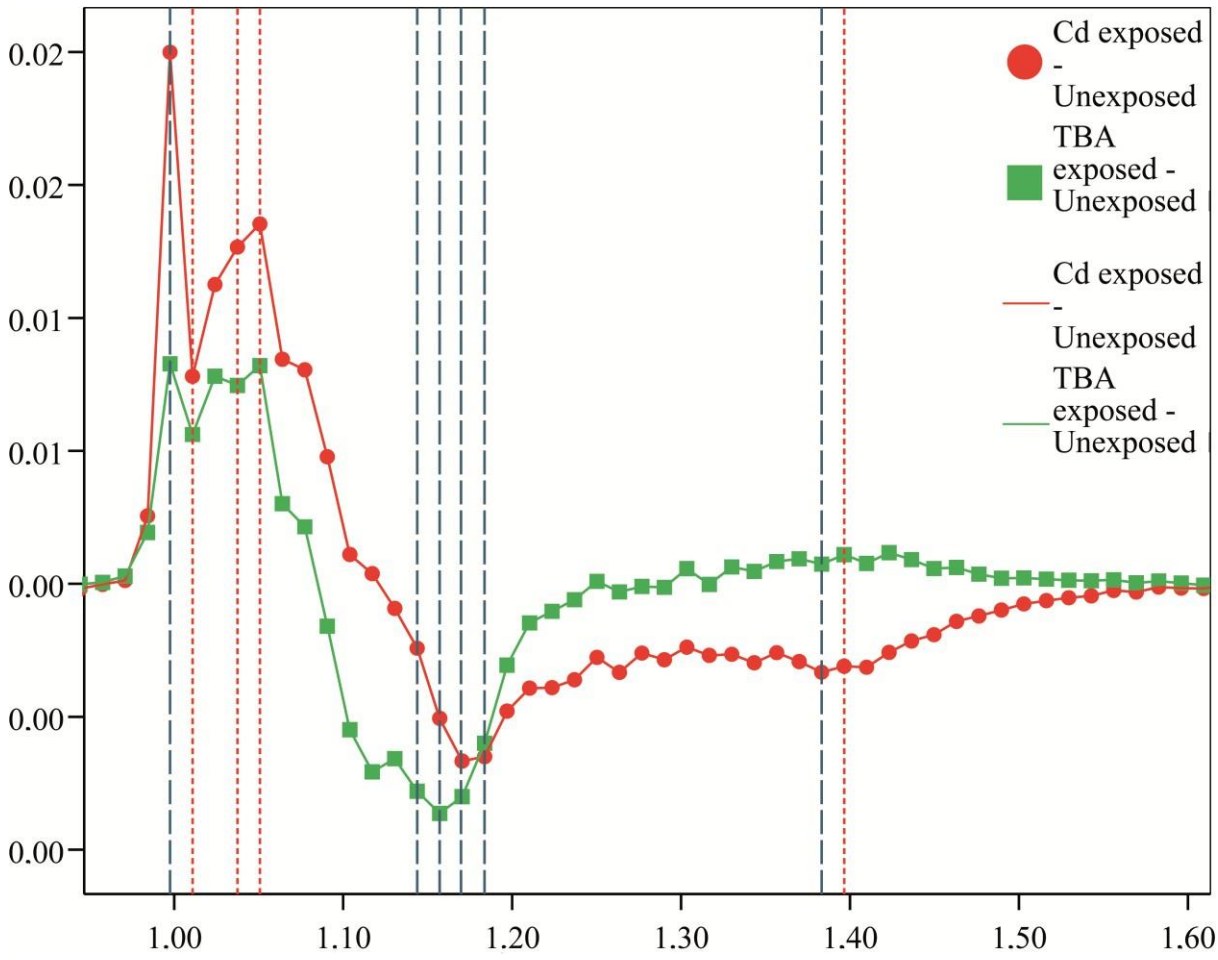

Fig. 4. Scatter plot of the differences among the means of the frequencies of Cd exposed and TBA exposed with respect to unexposed fish (y axis) to LCFD (x axis), according to toxicants. The vertical dotted (red)/dashed (blue) lines demonstrates the frequency values of LCFD enhancing the differences among classes. The dotted (red) vertical lines refer to values selected by means of linear discriminant stepwise analysis.

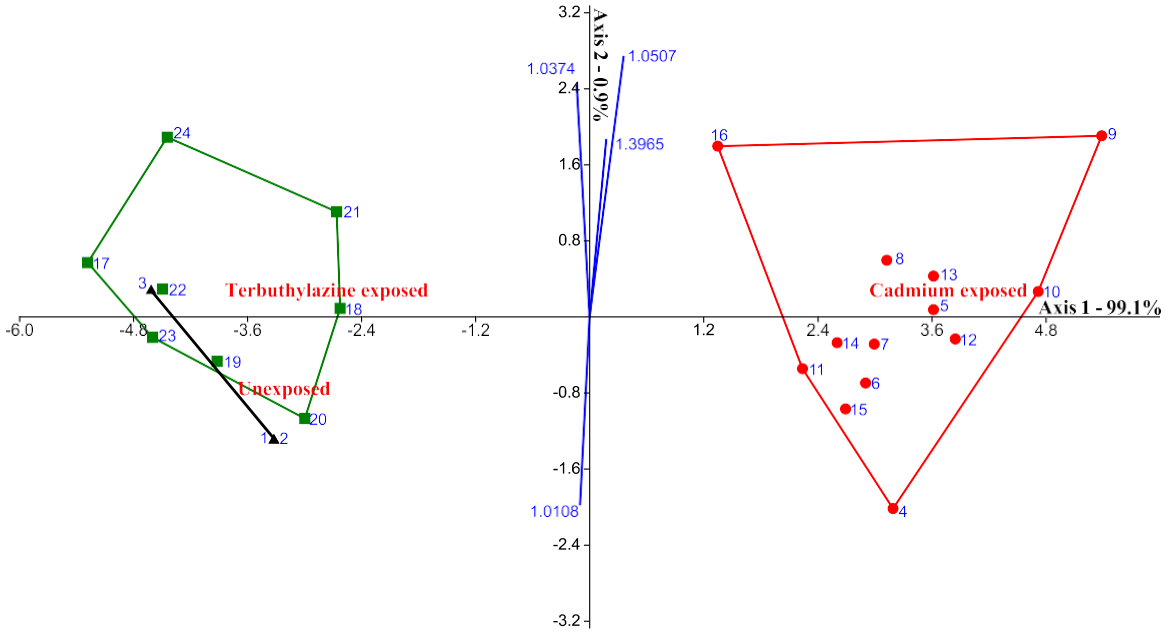

Fig. 5. CVA plot. Note the clear separation of exposure class along axis 1 by means of convex hull polygons. As predicted by the model, false positive n. 3 is enclosed in the convex polygon of TBA exposed cases. The LCFDs corresponding to the frequencies selected by means of linear discriminant stepwise analysis are reported as vectors.